Nano Research 2016, 9(7): 2138–2148
DOI 10.1007/s12274-016-1103-0
Research Article
ISSN 1998-0124
CN 11-5974/O4

Plasma-induced nanowelding of a copper nanowire network and its application in transparent electrodes and stretchable conductors

Ranran Wang, Haitao Zhai, Tao Wang, Xiao Wang, Yin Cheng, Liangjing Shi, and Jing Sun (✉)

The State Key Lab of High Performance Ceramics and Superfine Microstructure, Shanghai Institute of Ceramics, Chinese Academy of Sciences, 1295 Dingxi Road, Shanghai 200050, China

Received: 2 February 2016
Revised: 13 April 2016
Accepted: 16 April 2016

KEYWORDS
plasma,
nanowelding,
transparent electrode,
stretchable conductor,
organic solar cell

ABSTRACT

Copper nanowires (Cu NWs) have attracted increasing attention as building blocks for electronics due to their outstanding electrical properties and low cost. However, organic residues and oxide layers ubiquitously existing on the surface of Cu NWs impede good inter-wire contact. Commonly used methods such as thermal annealing and acid treatment often lead to nanowire damage. Herein, hydrogen plasma treatment at room temperature has been demonstrated to be effective for simultaneous surface cleaning and selective welding of Cu NWs at junctions. Transparent electrodes with excellent optical-electrical performance (19 $\Omega \cdot sq^{-1}$ @ 90% T) and enhanced stability have been fabricated and integrated into organic solar cells. Besides, Cu NW conductors with superior stretchability and cycling stability under stretching speeds of up to 400 $mm \cdot min^{-1}$ can also be produced by the nanowelding process, and the feasibility of their application in stretchable LED circuits has been demonstrated.

1 Introduction

Many modern devices including touch screens, organic light-emitting diodes (OLEDs), and electronic displays require transparent electrodes with high conductivity [1–4]. Currently, indium tin oxide (ITO) films are most commonly used in industry due to their excellent transparency (~90% at 550 nm) and low sheet resistance (~20 $\Omega \cdot sq^{-1}$). However, the rising cost and brittleness of ITO make it urgent to explore alternatives satisfying the massive demand for flexible devices. Carbon-based (i.e., carbon nanotubes (CNTs) and graphene) [5–8] and metal nanostructures (i.e., metal nanowires and nanogrids) [9–12] have been extensively used to fabricate transparent conductors in the last several years. However, the performance of transparent conductors based on CNTs and graphene often cannot meet the requirements of many applications, and the high price of noble metals (Au and Ag) makes them uncompetitive for large-area usage even though they can exhibit superior conductivity and transmittance. Recently, copper nanowires (Cu NWs) have attracted

Address correspondence to jingsun@mail.sic.ac.cn

considerable attention as an alternative for future transparent conductors, since their electrical conductivity is comparable to that of silver, while the price is 100 times lower [13–15].

To produce transparent Cu NW electrodes with high performance, post-processing treatment is necessary to clean up residual organics and oxide layers on the surface, since their presence would dramatically increase the sheet resistance. Annealing and chemical treatment are effective ways to decompose or rinse off organic molecules. Zhang et al. [16] heated Cu NW films at 300 ℃ under the protective atmosphere of forming gas (5% hydrogen, 95% nitrogen), while thermal annealing was applied in a vacuum oven at 200 ℃ in Peng's group [17]. Nevertheless, this technique is not applicable to many flexible substrates. Several latest studies reported that rinsing Cu NW films with acid, i.e., acetic acid and lactic acid, could effectively remove both the organic capping molecules and the surface oxide/hydroxide, allowing direct contact between the nanowires [18–20]. This chemical approach enabled the fabrication of transparent electrodes with excellent properties (55 $\Omega \cdot sq^{-1}$ with 94% optical transmittance at 550 nm) at room temperature. Unfortunately, Cu NW films that underwent acid treatment became more easily oxidized.

In addition to surface cleaning, welding is another route to decrease the contact resistance. Several methods including rapid thermal annealing [21], electrical sintering [22], mechanically assisted cold welding [23], and photo-thermal welding [24] have been successfully used to weld noble metal nanostructures. However, these methods did not show much success in the case of Cu NWs due to surface oxidation. Although Ko et al. [25] implemented slight nanowelding of Cu NW films via circularly polarized laser scanning, the resultant optical-electrical performance (5 $k\Omega \cdot sq^{-1}$ with 92% optical transmittance at 550 nm) was inferior to that of the high-rank transparent electrodes.

Herein, we present a plasma treatment technique, which enables effective removal of organic residues and surface oxides at room temperature, simultaneously inducing plasmonic nanowelding at the inter-wire junctions. Transparent electrodes with excellent performance (19 $\Omega \cdot sq^{-1}$ with 90% optical transmittance at 550 nm) and enhanced stability were obtained, outperforming previous reports. Organic solar cells were constructed to confirm the applicability of the resultant Cu NW transparent electrode. Besides, the nanowelding process was found to be advantageous for improving the stretchability of Cu NW networks, bringing out conductors with superior stretchability and cycling stability under stretching speeds of up to 400 $mm \cdot min^{-1}$. The feasibility of Cu NW conductors was demonstrated by fabricating stretchable LED circuits.

2 Experimental

2.1 Fabrication of Cu NW films

Cu NWs were synthesized following the procedure described in our previous work [26], and were fabricated into thin films using a vacuum filtration. Typically, Cu NWs were dispersed in toluene by bath sonication for 1–2 min and then filtered onto a nitrocellulose filter membrane. After that, the filter membranes were transferred onto glass slides or silicon wafers, dried under vacuum at 80 ℃ for 2 h, and then dipped in acetone for 30 min to dissolve the filtration membrane, leaving copper nanowire thin films on glass slides or silicon wafers.

2.2 Hydrogen plasma treatment

The inductively coupled plasma instrument was designed by the Institute of Plasma Physics of the Chinese Academy of Sciences. The treatment process started with evacuating the chamber loaded with Cu NW samples. Then, the chamber was filled with hydrogen to a pressure of 40–150 Pa. Purple plasma was generated upon application of voltage, and a power of 20 W was generally used in this work. Cu NW samples were treated by the plasma for 1–20 min and were subsequently taken out for characterization.

2.3 Polymer solar cell fabrication

In order to decrease the surface roughness, Cu NW films were first transferred to polyacrylate substrates [26]. A thin layer of TiO_2 nanoparticles was spin-cast as an electron transfer layer (ca. 30–40 nm). The substrate was then transferred into a glove-box, where a 200 nm thick photoactive layer was cast from

2.5 wt.% P3HT:PCBM (Rieke Metals, American Dye Source, 1:0.8 ratio) in 1,2-dichlorobenzene. The solvent was allowed to dry out after ~20 min in a covered petri dish. The active layer was further annealed at 130 ℃ for 10 min to remove the solvent completely. Deposition of the anode by thermal evaporation of MoO_3 (10 nm) and Ag (100 nm) under vacuum (2×10^{-3} Pa) completed the device fabrication.

2.4 Fabrication of stretchable Cu NW conductors

Ecoflex (smooth on) elastomer substrates were obtained by mixing ingredients A and B in a 1:1 weight ratio and subsequent polymerization at 40 ℃ for 30 min. The substrates were then stretched to 100% strain and fixed on aluminum alloy wafers. Plasma-treated Cu NW films on silicon wafers were then transferred to the pre-strained elastomer substrates and kept in a vacuum oven at 80 ℃ for another 30 min. After peeling off silicon wafers and releasing the elastomer substrates, Cu NW conductors were obtained.

2.5 Characterization

Scanning electron microscopy (SEM) characterization was accomplished using a Hitachi SU8200 FE-SEM instrument. Micro-Raman testing was performed with a DXR Raman Microscope (Thermal Scientific Corporation, USA) with a 532 nm excitation length. The sheet resistance of the electrodes was measured using a four-point probe resistivity meter (Loresta EP MCP-T360, Mitsubishi Chemical, Japan). The transmittance of the Cu NW electrodes was measured on a UV–vis spectrometer (Lambda 950, Perkin-Elmer, Shelton, USA). The stretching of Cu NW conductors was performed on a moving stage, and the resistance change was measured by an electrochemical workstation (PARSTAT 2273, Princeton Applied Research).

3 Results and discussion

3.1 Plasma-induced nanowelding of Cu NWs

Cu NWs were synthesized using a modified liquid ammonium method proposed in our previous work [26]. Most of the nanowires had a diameter of 60–100 nm, and a length of over 50 μm. They were dispersed in toluene and made into thin films on glass or elastomer substrate using vacuum filtration. The as-prepared films showed poor electrical conductivity, since Cu NWs were isolated by residual organics and oxide layers on the nanowire surface and could not form conducting paths, as shown in Fig. 1. The inductively coupled hydrogen plasma was subsequently used to treat the sample and enhance the inter-nanowire contact. Experimental details for the hydrogen plasma treatment can be found in the abovementioned methods. The Cu NW films before and after hydrogen plasma treatment were characterized by scanning electron microscopy, transmission electron microscopy (TEM), Raman spectroscopy, and electrical resistance measurements. Figures 2(a)–2(c) show plan view SEM images of Cu NW films before and after treatment. Organic residues originating from the synthesis process were observed in the sample before treatment, which was reflected in the rough surface of nanowires and a film-like substance wrapped around the nanowire junctions, as marked by a red circle. Figure S1 in the Electronic Supplementary Material (ESM) shows the tilted SEM images of Cu NW films, where a layer of organic molecules wrapping

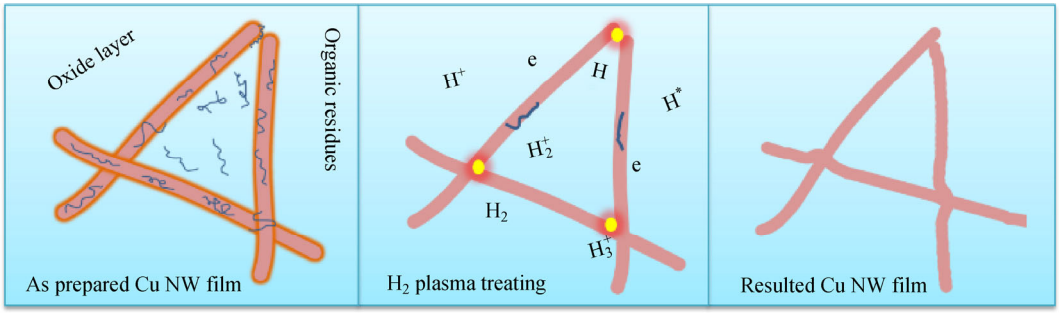

Figure 1 Schematic illustration of the hydrogen plasma treatment process.

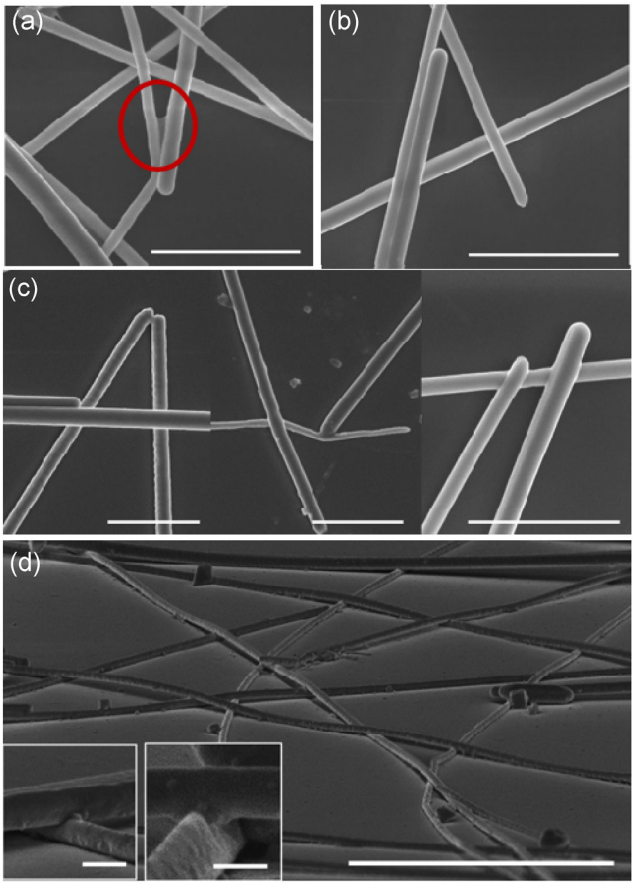

Figure 2 SEM images of Cu NW films before and after plasma treatment. (a) Plan view SEM image of Cu NW network before treatment. Scale bar: 1 μm. (b) Plan view SEM image of Cu NW network after plasma treatment for 3 min. Scale bar: 1 μm. (c) Plan view SEM image of Cu NW network after plasma treatment for 10 min. Scale bar: 1 μm. (d) Tilted SEM image of the sample shown in (c), scale bars are 200 nm, 100 nm, and 3 μm from left to right, respectively.

around nanowires can be clearly observed, hindering the inter-nanowire contact at junctions. After hydrogen plasma treatment for 3 min, the organic molecules were removed, and a good ohmic contact at the Cu NW junctions formed. Moreover, at increased treatment time, welding was observed at inter-wire junctions, head-to-head joints, head-to-side joints, or even between nanowires placed side by side, as seen in Fig. 2(c). Figure 2(d) shows a tilted SEM image of the Cu NW film after plasma treatment, with contacts of different morphologies formed at inter-wire junctions. In one case, the top nanowires dented to facilitate the intercalation of the bottom ones, while in the other case, the top nanowires deformed towards the bottom ones, forming enfolded contact morphology.

The nanowelding of Cu NWs during plasma treatment was mainly attributed to two factors. First, the etching and reductive effects of hydrogen plasma produced clean surfaces of Cu NWs. As reported by Lou [23], a clean surface under high vacuum is a primary factor for the diffusion of metal atoms on the surface, and Cu NW films in the plasma chamber clearly satisfied this requirement.

It was also pointed out that the diffusion barrier for a single metal atom on the surface is quite low (typically less than 1 eV). However, creating isolated atoms has a much higher energy cost. In this work, surface plasma enhanced photo thermal provided the extra energy required, which was the second factor. It is well recognized that light waves can induce a heating effect, which has been used in a range of applications [27, 28]. During the process of glow discharge hydrogen plasma treatment, intense purple light (>1 $W \cdot cm^{-2}$) was generated due to the electron transitions from activated (H^*, H_2^*) to ground states (H, H_2). The emission spectrum of hydrogen plasma is covered in previous reports [29–31]. In addition to the base peak at 656.3 nm (Hα), strong peaks in the 570–610 nm band (H_2 molecule) were observed, close to the surface plasmon resonance peak of Cu NWs at 576 nm (obtained from extinction spectrum, Fig. S2 in the ESM). Therefore, the light intensity was greatly enhanced at the contact points of piled metal nanowires, due to the surface plasmonic resonance effect, and consequently caused confined thermal heating to achieve local nanowelding. As proposed by Garnett et al., the inter-wire spacing is essential for the field concentration effect, the heating rapidly becomes less effective once the wires touch, and the NWs cool as a result [24]. This self-limited welding process could provide unaffected nanowire morphology away from the junctions, whereas annealing caused either no melting or the undesired fragmentation of the nanowires. A series of annealing experiments was performed under a protective atmosphere of hydrogen at temperatures from 200 to 400 ℃. Obvious welding of our Cu NWs would not occur until the temperature exceeded 230 ℃, nevertheless, welding was implemented at room temperature via hydrogen plasma treatment due to the aforementioned two factors.

To understand the nature of the Cu NW welding process, selected area electron diffraction (SAED) and high resolution TEM analysis were conducted. Figure 3 shows a high resolution TEM image of two nanowires placed side by side after plasma treatment for 10 min. The two nanowires were welded without any gap, with their fringes matching perfectly and not exhibiting any defective interface area. The same orientation of the two nanowires may facilitate interfacial welding, which has been proposed in the "orientated-attachment" mechanism [32, 33].

The oxidation state of Cu NWs was characterized by Raman spectroscopy. Due to their high activity, Cu NWs are prone to oxidation when exposed to air. As shown in Fig. S3 in the ESM, Cu_2O (~220, 411 cm^{-1}) and CuO (~289, 494, 621 cm^{-1}) were present in Cu NW films before treatment, with Cu_2O being the dominant oxide, in agreement with previous reports [34, 35]. As can be seen, the Cu oxidation state varied at different sections of NW films, therefore, three distinct points were characterized for each sample to ensure accuracy of analysis. After hydrogen plasma treatment, the signals of oxides were strongly weakened, and the peaks ascribed to CuO disappeared after 10 min of treatment. After 15 min, almost no oxide peaks were observed, in line with the efficient reduction effect of hydrogen plasma, which promised clean Cu NW surfaces.

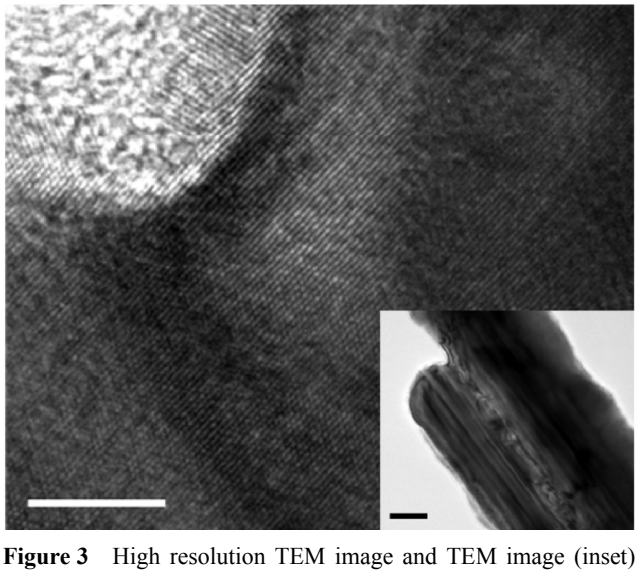

Figure 3 High resolution TEM image and TEM image (inset) of two nanowires placed side by side after plasma treatment. Scale bars are 5 and 50 nm, respectively.

3.2 Transparent electrodes based on Cu NW networks

To demonstrate the practicality of our hydrogen plasma nanowelding process, transparent electrodes were fabricated using vacuum filtration and tested by a four point probe resistance meter. The initial sheet resistance of the Cu NW percolation network was generally above 10^6 Ω·sq^{-1} due to the residual organics and oxide layers on the surface. This value decreased to several hundreds or thousands of Ω·sq^{-1} after plasma treatment for 3 min, mainly due to the surface cleaning effect, and then decreased to several tens of Ω·sq^{-1}, depending on the network density, when the treatment time was increased to 5 min. In addition to further removal of insulating residues, nanowelding of the inter-wire junctions was mainly responsible for the conductance improvement. Further treatment prolongation led to a slight decrease and then to an increase of the sheet resistance. Severe etching of Cu NWs was the main reason for the increase of the sheet resistance. Cu NW films with the same thickness were treated by hydrogen plasma to investigate the influence of hydrogen pressure. As shown in Fig. 4(b), in the 0–100 Pa range, higher pressure led to Cu NW electrodes with lower sheet resistance. Since more H_2 molecules will be ionized at increased pressure, the surface cleaning and nanowelding effects of Cu NWs will be intensified. Nevertheless, further elevation of the pressure gives rise to severe etching of Cu NWs, as shown in Fig. S4 in the ESM, leading to a higher sheet resistance of Cu NW electrodes. Therefore, a hydrogen pressure of 90 Pa was generally used in this work if not otherwise specified.

Figure 4(c) shows plots of transmittance (at 550 nm) versus the sheet resistance of Cu NW films that were subjected to different post-treatment processes. Sheet resistances as low as 19 and 11 Ω·sq^{-1} at transmittances of 90% and 86%, respectively, were obtained after hydrogen plasma treatment, being comparable to the corresponding ITO values, and outperforming most of the Cu NW electrodes reported. The figure of merit (FOM) specific value of DC conductivity (σ_{dc}) and optical conductivity (σ_{op}) is often used to evaluate the conductive performance of metal nanowire conductive films as applicable electrodes. A higher FOM represents

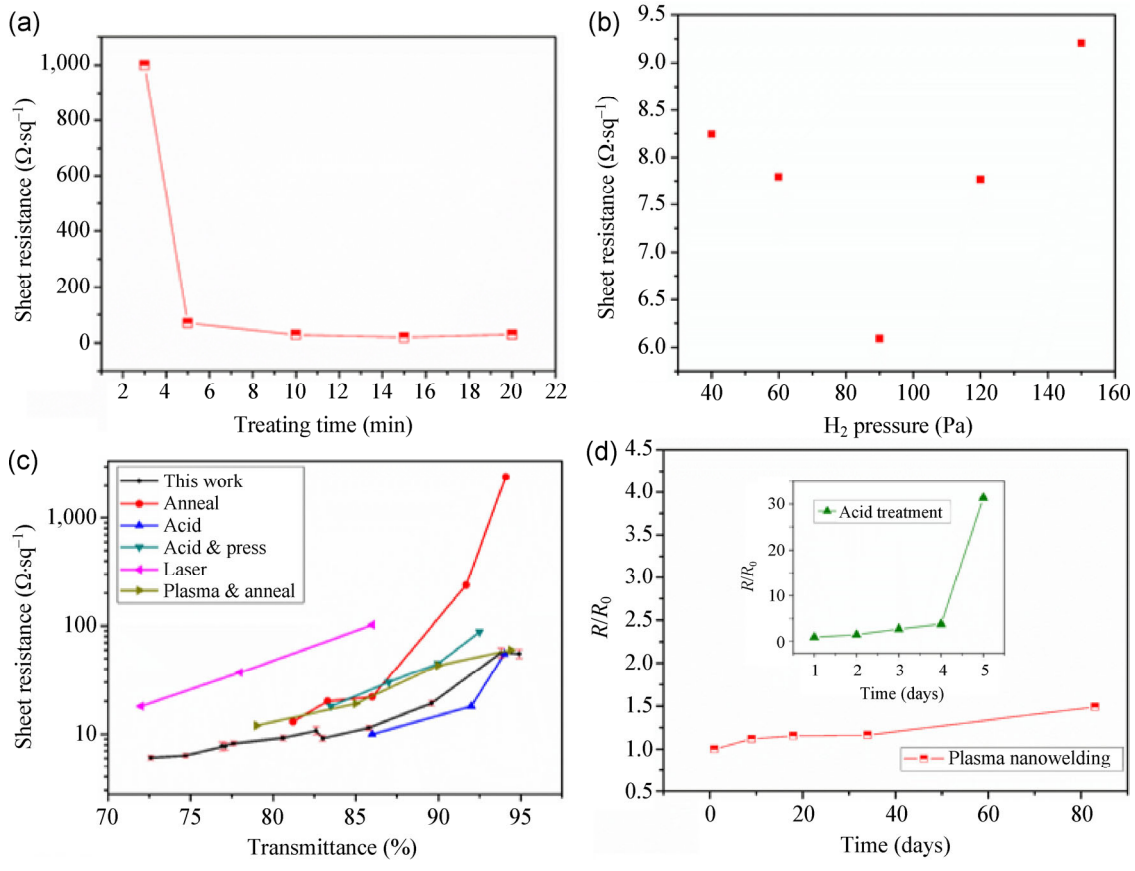

Figure 4 (a) Plot of sheet resistance versus hydrogen plasma treatment time. (b) Sheet resistance change versus hydrogen pressure. (c) Comparison of sheet resistance and optical transmittance of Cu NW films treated by hydrogen plasma with those annealed under hydrogen, treated with acid [18], acid and press [19], laser scanning [24], and H_2/Ar plasma combined with annealing [14]. (d) Sheet resistance change (R/R_0) with time of Cu NW films treated by hydrogen plasma and lactic acid.

lower sheet resistance at higher transmittance, which is preferred in transparent conductive films.

$$T = (1 + 188.5/R_S \cdot \sigma_{op}/\sigma_{dc})^{-2} \quad (1)$$

According to Eq. (1), the FOM value of Cu NW films treated by hydrogen plasma was 218.9, much higher than that of the annealed Cu NW films (109.4). Such a high value can be attributed to a large aspect ratio of the in-house made nanowires, as well as to the efficient surface cleaning and nanowelding effect of hydrogen plasma treatment. Although surface cleaning and welding can also be implemented by annealing, the undesired fragmentation of Cu NWs significantly decreased the electrical conductance of the percolation network. Besides, annealing is not applicable to plastic substrates. Laser scanning has been proved to be effective for improving the conductance of Cu NW films at room temperature via plasmonic nanowelding. Unfortunately, the resulting optical-electrical performance (~102 Ω·sq^{-1} at a transmittance of 86%) lagged far behind the top-rank transparent electrodes, and could not meet the requirements of many electronic devices, such as solar cells and organic light-emitting diodes. Acid treatment could clean the surface of Cu NWs within 1 min and provide good ohmic contact at nanowire junctions, resulting in excellent optical-electrical performance (55 Ω·sq^{-1} at a transmittance of 94%). However, Cu NW electrodes were easily oxidized after acid treatment and lost conductance within several days of exposure to air.

On the contrary, electrodes treated with hydrogen plasma were stable ($R/R_0 \leqslant 2$) in air for at least two months, as seen from Fig. 4(d). According to our previous research, oxidation is easier at junctions and

broken fragments [36]. As to the acid-treated Cu NW films, oxide layers formed quickly at junctions, blocking the electron transport and resulting in loss of conductance. In the welded nanowire network, the electrons can still be transported through the welded junctions despite the oxide layers formed on the surface, which explains the good stability of Cu NW electrodes treated by hydrogen plasma.

3.3 Organic solar cells based on Cu NW transparent electrodes

Due to their superior optical-electrical performance, Cu NW thin films are competitive candidates to replace transparent ITO electrodes in organic solar cells. One of the obstacles to the usage of nanowire electrodes is their greater surface roughness. Herein, an *in situ* polymerization-transfer method was used to decrease the roughness of Cu NW based electrodes [37]. Briefly, the Cu NWs were deposited onto glass slides by vacuum filtration, with subsequent coating with vinyl monomers followed by *in situ* photochemically initiated polymerization. After peeling off, the resulting composite electrode was obtained. Figures S5(a) and S5(b) in the ESM show the 3D topographical images of the Cu NW/glass slide and the composite electrodes. The nanowire network was partially embedded into the polymer substrate of the composite electrode, unlike the glass electrode, where the nanowires stacked on top. Therefore, the bumps created by wire–wire junctions were counterweighed by polymer coverage, and the problem of protruding was resolved. Despite being embedded in polymers, the nanowires were connected, providing an intact conductive network. Thus, the sheet resistance showed no obvious change after transfer. Besides, the transmittance of the polymer substrate (~91%) is similar to that of the glass slide (92%), not sacrificing the transit of light. Figure S5(c) in the ESM shows that the height of the cross junction was much lower than the sum of the heights of two single nanowires. This result again indicated that two nanowires were not simply touching at the junction, but indeed welded together.

In addition to improved surface smoothness, the Cu NW/polymer composite electrodes were also mechanically robust. Negligible change of the sheet resistance was observed after the tape test, bath sonication, and ozone treatment. Inverted organic solar cells based on the Cu NW/polymer composite electrode were constructed. Briefly, a thin layer of TiO_2 nanoparticles was spin-cast as the electron transfer layer, followed by a 200 nm thick P3HT:PCBM photoactive layer. No obvious change of the Cu NW electrode sheet resistance was found after casting of the TiO_2 layer. Figure 5 shows a photograph and characteristic *I–V* curves of solar cells with the Cu NW/polymer composite film as a transparent electrode. A power conversion efficiency of 2.67%, with V_{oc} = 0.54 V, J_{sc} = 9.51 mA·cm^{-2}, and FF = 52% was obtained when plasma-treated Cu NW film was used as a transparent electrode. V_{oc}: open-circuit voltage; J_{sc}: short-circuit current density; FF: fill factor. This performance was superior to that of the device having an annealed Cu NW transparent electrode, which exhibited a power conversion efficiency of 2.52%, with V_{oc} = 0.53 V, J_{sc} = 9.2 mA·cm^{-2}, and FF = 52%. The higher short circuit current was mainly attributed to the superior optical- electrical performance of the plasma-treated Cu NW electrode. Unfortunately, its performance was still inferior to that of the ITO-based device, which had a power conversion efficiency of 3.5%, with V_{oc} = 0.59 V, J_{sc} = 9.62 mA·cm^{-2}, and FF = 62%. Although the surface roughness of the Cu NW electrode was improved by the polymer cover, it was still larger than that of ITO. The greater roughness lowered the film quality of the photo-active layer significantly, being mainly responsible for the low FF. Further perfection of the homogeneity

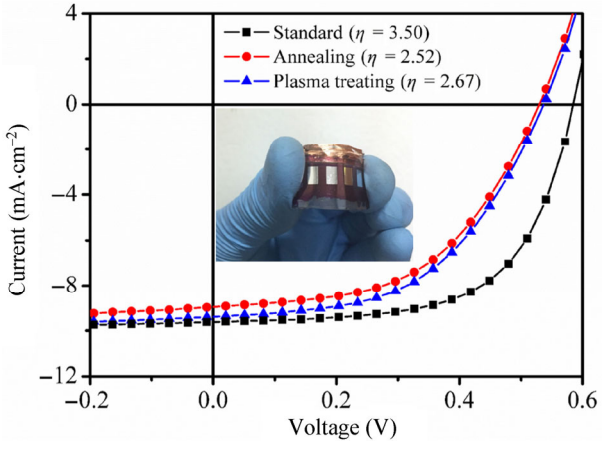

Figure 5 Characteristic *I–V* curves of solar cells with ITO and Cu NW films as transparent electrodes.

and smoothness of Cu NW electrodes will lead to better performance of the photovoltaic devices. Besides, the low cost and flexibility impart Cu NW based transparent electrodes superiority to ITO in commercial applications.

3.4 Stretchable Cu NW conductors and demonstration of stretchable LED circuits

Superior conductivity and stability, as well as nanowelding enhanced the mechanical robustness of Cu NW films, allowing their application in stretchable electronics as highly stretchable conductors. To prepare the latter materials, Cu NW films were fabricated using vacuum filtration with subsequent hydrogen plasma treatment and then transferred to pre-strained (100%) highly stretchable elastomer substrates (Ecoflex). The as-obtained stretchable conductor was fixed onto a moving stage and connected to a current–voltage measurement device using liquid metal (gallium) and copper wires. The electrical resistance was measured under various tensile strains. Figure 6(a) shows the photographs and optical microscopy images of stretchable Cu NW conductors at various tensile strains. Cu NW films with wavy structures firmly adhered to the elastomer substrates, and were not destroyed by the tape test and scratching with tweezers. The wavy structure was formed due to the out-of plane buckling of nanowelded Cu NWs during the release of pre-strained elastomer substrate. No debonding or cracks between the Cu NW/elastomer substrate and inside the Cu NW films were observed. In comparison, conductors based on acid-treated Cu NW films did not exhibit wavy structures with such large amplitude (Fig. S6 in the ESM), since the contact between nanowires in the acid treated sample was loose, allowing them to slide during the release of the substrates to a certain extent, rather than buckling out of plane like the welded nanowire network. The amplitude of the waves decreased gradually on stretching and flattened at 100% strain. Beyond 100% strain, the Cu NW networks deformed along the stretching direction, and a small number of micro-cracks were observed at 150% strain. The size and number of micro-cracks increased gradually on further stretching, and inter-connected Cu NW islands formed when the substrate was stretched to 250% strain.

Figure 6(b) shows the sheet resistance change of Cu NW conductors with stretching. Although the thickness was kept the same, Cu NW conductors that experienced different post-treatment exhibited different resistance, with the lactic acid treated sample exhibiting the highest initial resistance (R_0), ca. 12.6 Ω (measuring distance ~1 cm), and the samples treated by hydrogen plasma for 5 and 10 min exhibiting resistances of 3.1 and 1.6 Ω, respectively. Low resistance is the primary requirement for good conductors, which is better met by hydrogen plasma treated Cu NW samples than those treated by numerous other methods [24, 25]. When stretched, the acid-treated Cu NW conductor showed rapid degradation, with its resistance exceeding 1,000 Ω at 120% strain. On the contrary, Cu NW conductors treated by hydrogen plasma showed negligible resistance change up to 150% strain. After that, the resistance increased gradually due to the formation of micro-cracks. The resistances increased to 48.8 and 17.9 Ω at 250% strain, and the normalized resistances (R/R_0) were 15.7 and 11.2 for the 5 and 10 min samples, respectively. Notwithstanding a 10-fold increase, a resistance lower than 20 Ω is still acceptable for many electronic devices with high internal resistance. Figure 6(c) shows the cyclic performance of stretchable Cu NW conductors at different strains, indicating excellent electrical functionalities and stretching stability.

Stretching speed is an all-important indicator for the practical application of stretchable conductors. Unfortunately, most of the previous research did not specify the stretching speed used. Hu et al. [38] disclosed that the stretching performance of Cu NW-PU transparent conductors apparently deteriorates with increasing stretching speed. Herein, our Cu NW conductors maintained stable performance with increasing stretching speeds up to 400 mm·min^{-1} within 150% strain. Above 150% strain, the resistances after stretching were larger at higher stretching speeds, which was mainly attributed to the formation of micro-cracks. The stretchable Cu NW conductor was applied as a connector between a commercial LED lamp and the current–voltage measurement device. The video of the LED lamp demonstration using stretchable conductors at different stretching speeds is provided in the supplementary information. No degradation of

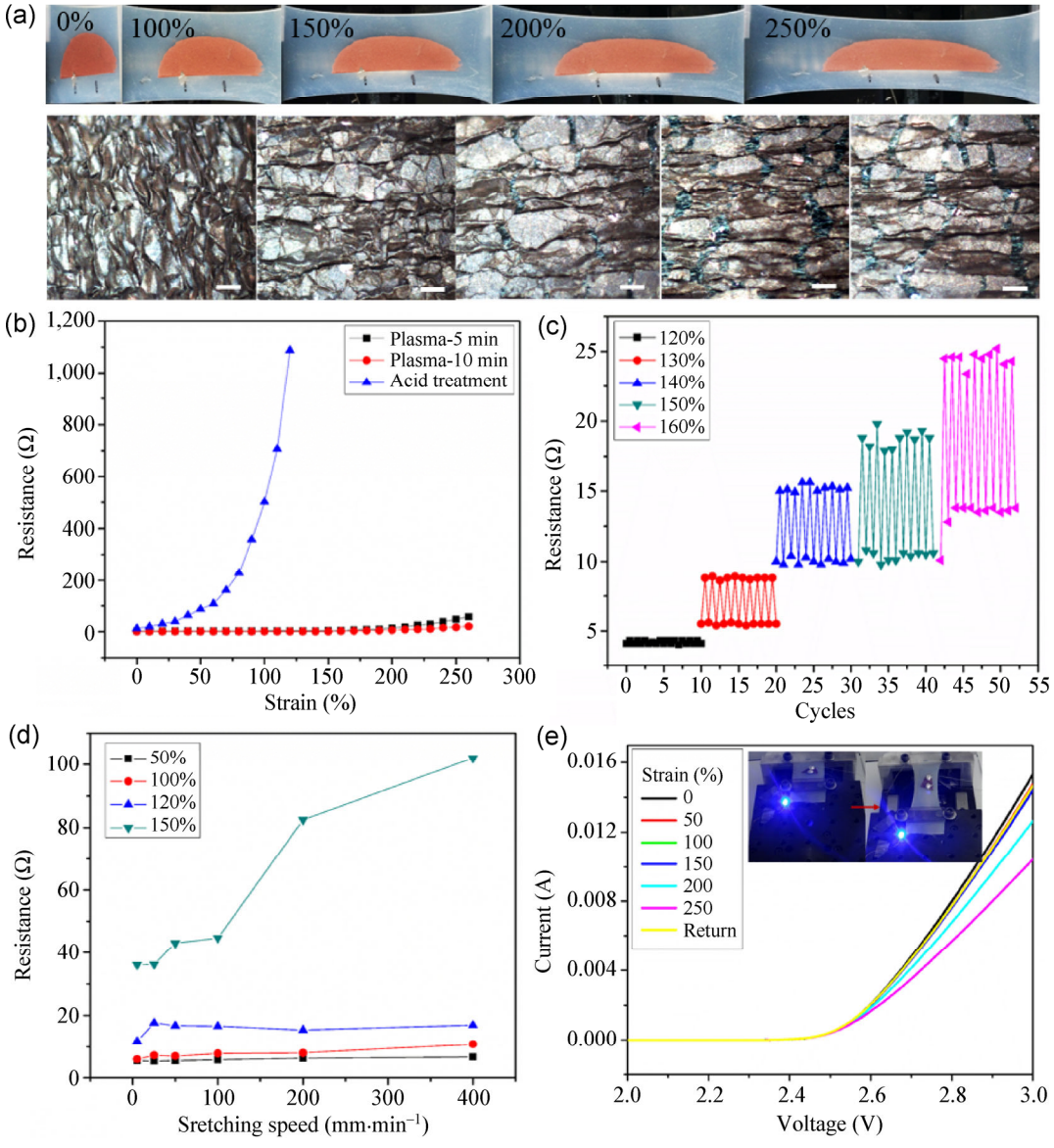

Figure 6 (a) Photographs and optical microscopy images of stretchable Cu NW conductors at different strains. Scale bar: 10 μm. (b) Resistance change measurement under various strains of Cu NW conductors on pre-strained elastomer substrates. (c) Cyclic test of stretchable Cu NW conductors under various strains. (d) Resistance change after stretching to different strains under various stretching speed. (e) Current–voltage measurement of LED lamps connected by stretchable Cu NW conductors at various strains. Insets are digital photos of the whole setup at 0% strain and 250% strain.

brightness was observed when the conductor was stretched to 130% strain with increasing the speed up to 400 mm min^{-1}. Figure 6(e) shows the *I*–*V* curve and the setup of the integrated circuits before and after stretching. Light was turned on when the applied voltage was greater than 2.5 V, and only slight degradation of the current was observed upon stretching to 150% strain. The brightness degradation was negligible even at ~250% strain due to the electrical and mechanical robustness of the stretchable conductor.

4 Conclusions

In summary, we have demonstrated a method utilizing hydrogen plasma for simultaneous surface cleaning and selective welding of Cu NWs at room temperature by taking advantage of the etching and reduction

effect of the plasma and localized field concentration offered by plasmonics. This opens up a new, simple, large-area scheme for low-temperature welding of metal nanostructures. Removal of surface oxides and organic residues, as well as welding at junctions significantly improved the conductivity of the Cu NW network. Transparent electrodes with excellent optical-electrical performance (19 $\Omega \cdot sq^{-1}$ @ 90% T, 11 $\Omega \cdot sq^{-1}$ @ 86% T) and enhanced stability have been fabricated and integrated into organic solar cells. Besides, the nanowelding process found its advantage in improving the stretchability of Cu NW networks, producing conductors with superior stretchability and cycling stability under stretching speeds of up to 400 $mm \cdot min^{-1}$. We demonstrated the feasibility of Cu NW conductors by fabricating stretchable LED circuits. We believe that the hydrogen plasma nanowelding process and the designed transparent electrodes and stretchable conductors may find use in intelligent and multifunctional soft electronics.

Acknowledgements

This work was financially supported by the National Basic Research Program of China (No. 2012CB932303), the National Natural Science Foundation of China (No. 61301036), Shanghai Municipal Natural Science Foundation (No. 13ZR1463600), and the Innovation Project of Shanghai Institute of Ceramics.

Electronic Supplementary Material: Supplementary material (SEM images, extinction spectrum, Raman spectra, AFM imaging, and optical microscope images) is available in the online version of this article at http://dx.doi.org/10.1007/s12274-016-1103-0.

References

[1] Kim, J.; Yun, J. H.; Kim, H.; Cho, Y.; Park, H. H.; Kumar, M. M. D.; Yi, J.; Anderson, W. A.; Kim, D. W. Transparent conductor-embedding nanocones for selective emitters: Optical and electrical improvements of Si solar cells. *Sci. Rep.* **2015**, *5*, 9256.

[2] Yao, S. S.; Zhu, Y. Nanomaterial-enabled stretchable conductors: Strategies, materials and devices. *Adv. Mater.* **2015**, *27*, 1480–1511.

[3] Chang, J. H.; Chiang, K. M.; Kang, H. W.; Chi, W. J.; Chang, J. H.; Wu, C. I.; Lin, H. W. A solution-processed molybdenum oxide treated silver nanowire network: A highly conductive transparent conducting electrode with superior mechanical and hole injection properties. *Nanoscale* **2015**, *7*, 4572–4579.

[4] Jin, Y. X.; Li, L.; Cheng, Y. R.; Kong, L. Q.; Pei, Q. B.; Xiao, F. Cohesively enhanced conductivity and adhesion of flexible silver nanowire networks by biocompatible polymer sol–gel transition. *Adv. Funct. Mater.* **2015**, *25*, 1581–1587.

[5] Kholmanov, I. N.; Magnuson, C. W.; Piner, R.; Kim, J. Y.; Aliev, A. E.; Tan, C.; Kim, T. Y.; Zakhidov, A. A.; Sberveglieri, G.; Baughman, R. H. et al. Optical, electrical, and electromechanical properties of hybrid graphene/carbon nanotube films. *Adv. Mater.* **2015**, *27*, 3053–3059.

[6] Lin, Y.; Kim, J. W.; Connell, J. W.; Lebrón-Colón, M.; Siochi, E. J. Purification of carbon nanotube sheets. *Adv. Eng. Mater.* **2015**, *17*, 674–688.

[7] Jurewicz, I.; Fahimi, A.; Lyons, P. E.; Smith, R. J.; Cann, M.; Large, M. L.; Tian, M. W.; Coleman, J. N.; Dalton, A. B. Insulator-conductor type transitions in graphene-modified silver nanowire networks: A route to inexpensive transparent conductors. *Adv. Funct. Mater.* **2014**, *24*, 7580–7587.

[8] Rahimi, S.; Tao, L.; Chowdhury, S. F.; Park, S.; Jouvray, A.; Buttress, S.; Rupesinghe, N.; Teo, K.; Akinwande, D. Toward 300 mm wafer-scalable high-performance polycrystalline chemical vapor deposited graphene transistors. *ACS Nano* **2014**, *8*, 10471–10479.

[9] Guo, C. F.; Ren, Z. F. Flexible transparent conductors based on metal nanowire networks. *Mater. Today* **2015**, *18*, 143–154.

[10] Song, J. Z.; Li, J. H.; Xu, J. Y.; Zeng, H. B. Superstable transparent conductive Cu@Cu4Ni nanowire elastomer composites against oxidation, bending, stretching, and twisting for flexible and stretchable optoelectronics. *Nano Lett.* **2014**, *14*, 6298–6305.

[11] Ye, S. R.; Rathmell, A. R.; Chen, Z. F.; Stewart, I. E.; Wiley, B. J. Metal nanowire networks: The next generation of transparent conductors. *Adv. Mater.* **2014**, *26*, 6670–6687.

[12] Lee, D.; Paeng, D.; Park, H. K.; Grigoropoulos, C. P. Vacuum-free, maskless patterning of Ni electrodes by laser reductive sintering of NiO nanoparticle ink and its application to transparent conductors. *ACS Nano* **2014**, *8*, 9807–9814.

[13] Mehta, R.; Chugh, S.; Chen, Z. H. Enhanced electrical and thermal conduction in graphene-encapsulated copper nanowires. *Nano Lett.* **2015**, *15*, 2024–2030.

[14] Rathmell, A. R.; Wiley, B. J. The synthesis and coating of long, thin copper nanowires to make flexible, transparent conducting films on plastic substrates. *Adv. Mater.* **2011**, *23*, 4798–4803.

[15] Rathmell, A. R.; Bergin, S. M.; Hua, Y. L.; Li, Z. Y.; Wiley, B. J. The growth mechanism of copper nanowires and their properties in flexible, transparent conducting films. *Adv. Mater.* **2010**, *22*, 3558–3563.

[16] Zhang, D. Q.; Wang, R. R.; Wen, M. C.; Weng, D.; Cui, X.; Sun, J.; Li, H. X.; Lu, Y. F. Synthesis of ultralong copper nanowires for high-performance transparent electrodes. *J. Am. Chem. Soc.* **2012**, *134*, 14283–14286.

[17] Guo, H. Z.; Lin, N.; Chen, Y. Z.; Wang, Z. W.; Xie, Q. S.; Zheng, T. C.; Gao, N.; Li, S. P.; Kang, J. Y.; Cai, D. J. et al. Copper nanowires as fully transparent conductive electrodes. *Sci. Rep.* **2013**, *3*, 9256.

[18] Mayousse, C.; Celle, C.; Carella, A.; Simonato, J.-P. Synthesis and purification of long copper nanowires. Application to high performance flexible transparent electrodes with and without PEDOT: PSS. *Nano Res.* **2014**, *7*, 315–324.

[19] Stewart, I. E.; Rathmell, A. R.; Yan, L.; Ye, S. R.; Flowers, P. F.; You, W.; Wiley, B. J. Solution-processed copper-nickel nanowire anodes for organic solar cells. *Nanoscale* **2014**, *6*, 5980–5988.

[20] Won, Y.; Kim, A.; Lee, D.; Yang, W.; Woo, K.; Jeong, S.; Moon, J. Annealing-free fabrication of highly oxidation-resistive copper nanowire composite conductors for photovoltaics. *NPG Asia Mater.* **2014**, *6*, e105.

[21] Oh, J. S.; Oh, J. S.; Shin, J. H.; Yeom, G. Y.; Kim, K. N. Nano-welding of Ag nanowires using rapid thermal annealing for transparent conductive films. *J. Nanosci. Nanotechnol.* **2015**, *15*, 8647–8651.

[22] Song, T.-B.; Chen, Y.; Chung, C.-H.; Yang, Y.; Bob, B.; Duan, H.-S.; Li, G.; Tu, K.-N.; Huang, Y.; Yang, Y. Nanoscale joule heating and electromigration enhanced ripening of silver nanowire contacts. *ACS Nano* **2014**, *8*, 2804–2811.

[23] Lu, Y.; Huang, J. Y.; Wang, C.; Sun, S. H.; Lou, J. Cold welding of ultrathin gold nanowires. *Nat. Nanotech.* **2010**, *5*, 218–224.

[24] Garnett, E. C.; Cai, W. S.; Cha, J. J.; Mahmood, F.; Connor, S. T.; Christoforo, M. G.; Cui, Y.; McGehee, M. D.; Brongersma, M. L. Self-limited plasmonic welding of silver nanowire junctions. *Nat. Mater.* **2012**, *11*, 241–249.

[25] Han, S.; Hong, S.; Ham, J.; Yeo, J.; Lee, J.; Kang, B.; Lee, P.; Kwon, J.; Lee, S. S.; Yang, M.-Y. et al. Fast plasmonic laser nanowelding for a Cu-nanowire percolation network for flexible transparent conductors and stretchable electronics. *Adv. Mater.* **2014**, *26*, 5808–5814.

[26] Cheng, Y.; Wang, S. L.; Wang, R. R.; Sun, J.; Gao, L. Copper nanowire based transparent conductive films with high stability and superior stretchability. *J. Mater. Chem. C* **2014**, *2*, 5309–5316.

[27] Cao, L. Y.; Barsic, D. N.; Guichard, A. R.; Brongersma, M. L. Plasmon-assisted local temperature control to pattern individual semiconductor nanowires and carbon nanotubes. *Nano Lett.* **2007**, *7*, 3523–3527.

[28] Govorov, A. O.; Zhang, W.; Skeini, T.; Richardson, H.; Lee, J.; Kotov, N. A. Gold nanoparticle ensembles as heaters and actuators: Melting and collective plasmon resonances. *Nanoscale Res. Lett.* **2006**, *1*, 84–90.

[29] Dunaev, A. V. Survey of emission spectra of the plasma of chlorine, hydrogen chloride, argon, and hydrogen. *Russ. Microelectronics* **2015**, *44*, 173–177.

[30] Klement, P.; Feser, C.; Hanke, B.; von Maydell, K.; Agert, C. Correlation between optical emission spectroscopy of hydrogen/germane plasma and the Raman crystallinity factor of germanium layers. *Appl. Phys. Lett.* **2013**, *102*, 152109.

[31] Wu, M. Z.; Huang, T. Y.; Jin, C. G.; Zhuge, L. J.; Han, Q.; Wu, X. M. Effect of multiple frequency H_2/Ar plasma treatment on the optical, electrical, and structural properties of AZO films. *IEEE T. Plasma Sci.* **2014**, *42*, 3687–3690.

[32] van Huis, M. A.; Kunneman, L. T.; Overgaag, K.; Xu, Q.; Pandraud, G.; Zandbergen, H. W.; Vanmaekelbergh, D. Low-temperature nanocrystal unification through rotations and relaxations probed by *in situ* transmission electron microscopy. *Nano Lett.* **2008**, *8*, 3959–3963.

[33] Cho, K. S.; Talapin, D. V.; Gaschler, W.; Murray, C. B. Designing PbSe nanowires and nanorings through oriented attachment of nanoparticles. *J. Am. Chem. Soc.* **2005**, *127*, 7140–7147.

[34] Schriver, M.; Regan, W.; Gannett, W. J.; Zaniewski, A. M.; Crommie, M. F.; Zettl, A. Graphene as a long-term metal oxidation barrier: Worse than nothing. *ACS Nano* **2013**, *7*, 5763–5768.

[35] Zhou, F.; Li, Z. T.; Shenoy, G. J.; Li, L.; Liu, H. T. Enhanced room-temperature corrosion of copper in the presence of graphene. *ACS Nano* **2013**, *7*, 6939–6947.

[36] Shi, L. J.; Wang, R. R.; Zhai, H. T.; Liu, Y. Q.; Gao, L.; Sun, J. A long-term oxidation barrier for copper nanowires: Graphene says yes. *Phys. Chem. Chem. Phys.* **2015**, *17*, 4231–4236.

[37] Hu, W. L.; Niu, X. F.; Li, L.; Yun, S.; Yu, Z. B.; Pei, Q. B. Intrinsically stretchable transparent electrodes based on silver-nanowire-crosslinked-polyacrylate composites. *Nanotechnology* **2012**, *23*, 344002.

[38] Hu, W. L.; Wang, R. R.; Lu, Y. F.; Pei, Q. B. An elastomeric transparent composite electrode based on copper nanowires and polyurethane. *J. Mater. Chem. C* **2014**, *2*, 1298–1305.